Precambrian Research 172 (2009) 301–310

Contents lists available at ScienceDirect

Precambrian Research

journal homepage: www.elsevier.com/locate/precamres

Correlation of Sturtian diamictite successions in southern Australia and northwestern Tasmania by Re–Os black shale geochronology and the ambiguity of "Sturtian"-type diamictite–cap carbonate pairs as chronostratigraphic marker horizons

Brian Kendall[a,b,*], Robert A. Creaser[b], Clive R. Calver[c], Timothy D. Raub[d], David A.D. Evans[e]

[a] School of Earth and Space Exploration, Arizona State University, Tempe, AZ 85287-1404, USA
[b] Department of Earth and Atmospheric Sciences, University of Alberta, Edmonton, AB T6G 2E3, Canada
[c] Mineral Resources Tasmania, P.O. Box 56, Rosny Park, Tasmania 7018 Australia
[d] Division of Geological and Planetary Sciences, California Institute of Technology 170-25, Pasadena, CA 91125, USA
[e] Department of Geology and Geophysics, Yale University, New Haven, CT 06520-8109, USA

ARTICLE INFO

Article history:
Received 27 October 2008
Received in revised form 14 May 2009
Accepted 26 May 2009

Keywords:
Neoproterozoic
Sturtian
Black shale
Re–Os
Glaciation
Australia
Tasmania

ABSTRACT

Recent geochronological studies have raised concerns regarding the accuracy of regional and global correlations of Neoproterozoic sedimentary successions using relative dating methods such as carbon isotope chemostratigraphy and glaciogenic diamictite–cap carbonate lithological and geochemical characteristics. Precise and accurate radio-isotopic age constraints for Neoproterozoic sedimentary rocks thus remain a high priority for establishing a reliable Neoproterozoic chronostratigraphy. Here, we present a new Re–Os age of 640.7 ± 4.7 Ma from black shales of the upper Black River Dolomite (Togari Group, northwestern Tasmania) that represents a minimum age for deposition of the immediately underlying, diamictite-bearing Julius River Member. The upper Black River Dolomite Re–Os age is statistically identical to a Re–Os age of 643.0 ± 2.4 Ma previously determined for the Sturtian post-glacial Tindelpina Shale Member (Umberatana Group, Adelaide Rift Complex, southern Australia). Consistent with previous lithostratigraphic and stromatolite biostratigraphic evidence, the Re–Os ages suggest broadly coeval deposition of the Julius River Member and Sturtian diamictites and overlying organic-rich marine shales. Consideration of the Neoproterozoic geochronological database suggests that "Sturtian"-type diamictite–cap carbonate pairs cannot be used as chronostratigraphic marker horizons for global correlation of the Neoproterozoic rock record.

1. Introduction

Global and regional correlation of the Neoproterozoic rock record is significantly hampered by a sparse paleontological record and a general paucity of suitable igneous material for precise U–Pb zircon age determinations. Consequently, efforts at establishing a Neoproterozoic chronostratigraphy are largely based on chemostratigraphy (primarily $\delta^{13}C$ and $^{87}Sr/^{86}Sr$ from carbonates) and identification of distinctive lithological and geochemical characteristics of carbonates capping glaciogenic diamictites (e.g., Kaufman and Knoll, 1995; Kaufman et al., 1997; Kennedy et al., 1998; Jacobsen and Kaufman, 1999; Walter et al., 2000; Halverson et al., 2005, 2007; Halverson, 2006; Hoffman et al., 2007). Neoproterozoic global correlation schemes based on these methods commonly assume global ("Snowball Earth") or near-global ("Slushball Earth") glaciations at ca. 700 Ma ("Sturtian") and ca. 635 Ma ("Marinoan") and a glaciation of uncertain extent at ca. 580 Ma ("Gaskiers"). However, the number, timing, extent, and duration of Neoproterozoic glaciation remain an ongoing topic of debate (Fairchild and Kennedy, 2007), so the above tripartite division of Neoproterozoic glacial deposits may be erroneous. For example, Kendall et al. (2006) show that the archetypal "Sturtian" glaciation of southern Australia is significantly younger than ca. 685–750 Ma glaciogenic diamictites on other continents previously suggested as correlatives.

Carbon, sulfur, and strontium isotope chemostratigraphy are relative dating tools that do not unambiguously provide chronological information and thus require numerical calibration by independent radio-isotopic and biostratigraphic data to be useful for global correlation schemes (Meert, 2007). Neoproterozoic carbon isotope chemostratigraphic profiles for similar aged rocks can exhibit a sig-

* Corresponding author at: School of Earth and Space Exploration, Arizona State University, Tempe, AZ 85287-1404, USA. Fax: +1 480 965 8102.
E-mail address: brian.kendall@asu.edu (B. Kendall).

0301-9268/$ – see front matter © 2009 Elsevier B.V. All rights reserved.
doi:10.1016/j.precamres.2009.05.001

nificant degree of scatter both within and between cratonic blocks because of diagenetic alteration, incomplete stratigraphy, and surface-to-deep ocean $\delta^{13}C$ gradients (e.g., Melezhik et al., 2001; Knauth and Kennedy, 2005; Fairchild and Kennedy, 2007; Jiang et al., 2007; Giddings and Wallace, 2009). These problems complicate attempts at establishing useful composite regional and global chemostratigraphic profiles. Strontium isotope chemostratigraphy shows some promise for correlation of Neoproterozoic sedimentary successions because of a systematic rise in $^{87}Sr/^{86}Sr$ during the Neoproterozoic, but the $^{87}Sr/^{86}Sr$ curve requires significant improvements in sample resolution (Halverson et al., 2007) and will generally be an insensitive chronometer at timescales much shorter than the seawater Sr residence time ($\sim$ 2–3 M.y. for the modern ocean; Ravizza and Zachos, 2006). The resolution of the Neoproterozoic sulfur isotope record remains too coarse for detailed global chemostratigraphy, although some broad temporal trends appear preserved in some basins (e.g., Fike et al., 2006).

Thus, precise and accurate U–Pb zircon and Re–Os black shale ages remain a high priority for reliable regional and global correlations of the Neoproterozoic rock record. Radio-isotopic calibration of the Neoproterozoic geological timescale is still limited to a relatively small number of precise U–Pb zircon ages from volcanic rocks (Evans, 2000; Trindade and Macouin, 2007) and Re–Os ages from black shales (Kendall et al., 2004, 2006). Geochronology represents one critical test for distinguishing among hypotheses proposed to explain low-latitude Neoproterozoic glaciation, especially the hard "Snowball Earth" (Kirschvink, 1992; Hoffman and Schrag, 2002) and "Slushball Earth" (Hyde et al., 2000; Schrag and Hoffman, 2001) hypotheses predicting global and near-global synchronous glaciations, respectively, and the "Zipper-rift" hypothesis suggesting diachronous glaciation on uplifted rift margins associated with Rodinia breakup (Eyles and Januszczak, 2004). The "High Obliquity, Low-latitude Ice, STrong seasonality" (HOLIST) hypothesis would permit either synchronous or diachronous glaciation preferentially in low-latitudes (Williams, 2008), but this model has been challenged by both theoretical and empirical evidence (Maloof et al., 2002; Evans, 2006).

The likelihood of tectonic proximity between Western Tasmania and southern Australia during the Neoproterozoic Era has led to a number of attempts at correlating the Neoproterozoic rock records of these two regions (Calver, 1998; Burrett and Berry, 2000; Calver and Walter, 2000; Preiss, 2000; Karlstrom et al., 2001; Direen and Crawford, 2003; Meffre et al., 2004; Berry et al., 2008). However, correlation of the "Sturtian" (Yudnamutana Subgroup) and "Marinoan" (Yerelina Subgroup, including the Elatina Formation) glacial deposits of the Adelaide Rift Complex, southern Australia, with two diamictite intervals present within the Togari Group of northwestern Tasmania is hampered by the absence of precise radio-isotopic age constraints for some of the diamictite intervals (Calver, 1998; Preiss, 2000; Calver and Walter, 2000; Calver et al., 2004; Kendall et al., 2006). The Croles Hill Diamictite from the upper Togari Group, constrained to be younger than a U–Pb SHRIMP zircon age of 582 ± 4 Ma from underlying rhyodacite, is potentially correlative with the undated Elatina Formation (Calver and Walter, 2000; Calver et al., 2004). Similarly, Calver (1998) and Calver and Walter (2000) suggest deposition of the undated, diamictite-rich Julius River Member (upper Black River Dolomite, lower Togari Group) may be synchronous with Sturtian glaciogenic sedimentation between 659 ± 6 Ma (U–Pb SHRIMP zircon age from a tuffaceous bed within the lower Wilyerpa Formation, South Australia; Fanning and Link, 2008) and 643.0 ± 2.4 Ma (Re–Os black shale age from the post-glacial Tindelpina Shale Member; Kendall et al., 2006). Here, we present a new Re–Os black shale age for the upper Black River Dolomite that provides a minimum depositional age for underlying Julius River Member diamictites.

2. Togari Group, northwestern Tasmania

The paleogeographic position of the Western Tasmania Terrane in the Late Neoproterozoic is not well constrained, but this crustal block may have been connected to the East Antarctic margin of the Mawson continent before ca. 580 Ma (Berry et al., 2008); paleomagnetic evidence indicates western Tasmania was connected to East Gondwanaland by Cambro-Ordovician boundary time (Li et al., 1997). In the Smithton Synclinorium of northwestern Tasmania, an unconformity separates unmetamorphosed and gently deformed strata of the Togari Group from the underlying Rocky Cape Group (Fig. 1). Locally, the coarse-grained Forest Conglomerate defines the base of the Togari Group and is overlain by 600 m of stromatolitic dolostones, organic-rich chert and shale, and diamictite of the Black River Dolomite (Calver, 1998; Calver and Walter, 2000). Vase-shaped microfossils (remains of testate amoebae; Porter and Knoll, 2000) are preserved in chert facies of the lower Black River Dolomite (incorrectly termed Smithton Limestone by Saito et al., 1988).

Two lines of evidence suggest a $\leq$200 m thick diamictite interval (Julius River Member) in the upper Black River Dolomite may be correlative with the thick (up to 6 km) Sturtian glaciogenic diamictites of the lower Umberatana Group, Adelaide Rift Complex, southern Australia (Fig. 2): (1) iron formation is associated with both Sturtian diamictites (Preiss, 1990, 1993; Lottermoser and Ashley, 2000) and correlatives of the Julius River Member in western Tasmania (Calver, 1998), and (2) dolomite clasts within the Julius River Member contain the stromatolite *Baicalia burra* (Griffin and Preiss, 1976; Calver, 1998), that is also present within the pre-Sturtian Skillogalee Dolomite, Burra Group (Belperio, 1990; Preiss, 1990). Lithological (stromatolitic dolostone and organic-rich chert) and carbon isotope ($\delta^{13}C_{carb} \sim +2‰$ to +6‰) similarities may suggest correlation of the Skillogalee Dolomite and Black River Dolomite (Schidlowski et al., 1975; Veizer and Hoefs, 1976; Belperio, 1990; Calver, 1998).

In the North Flinders Zone and Baratta Trough of the Adelaide Rift Complex, the Sturtian glacial succession was deposited by sediment gravity flows contemporaneously with two glacial depositional cycles, with evidence of glaciation being preserved in the form of striated clasts and dropstones (e.g., Young and Gostin, 1991; Eyles et al., 2007). However, evidence of a glacial influence in the Julius River Member is not compelling because that diamictite unit comprises sub-rounded, intrabasinal, dolomitic clasts surrounded by a fine-grained, dolomitic mudstone matrix (Calver, 1998). At the type section in Julius River (Julius River, southern Arthur Forest, Tasmania), a $\sim$2 m dolostone clast-framework microbreccia with an organic-rich, dolomitic matrix separates structurally uncomplicated lower Black River dolostone from overlying black shale containing dolostone lonestones at the base of the Julius River Member. This unconformable microbreccia-defined contact may represent karst or regolith produced during subaerial exposure.

Pyritic, organic-rich shales with subordinate carbonate conformably overlie the Julius River Member and comprise the top of the Black River Dolomite. The shale-carbonate succession is lithologically similar to the basal Tindelpina Shale Member of the Tapley Hill Formation that overlies most Sturtian glaciogenic deposits in the Adelaide Rift Complex (Calver, 1998; Calver and Walter, 2000). The Black River Dolomite is succeeded by the 1 km thick Kannunah Subgroup that comprises a basal unit of fine-grained siliciclastics and volcaniclastic arenites (Keppel Creek Formation) overlain by rhyodacite and diamictite (250 m thick Croles Hill Diamictite) (Calver et al., 2004). The latter contains thin, fine-grained dropstone-bearing intervals that suggest a possible glacial imprint during deposition. The Croles Hill Diamictite is not overlain by a distinctive cap carbonate, but rather by 10–50 m of red mudstone and more than 200 m of tholeiitic basalt (Spinks Creek Volcanics)

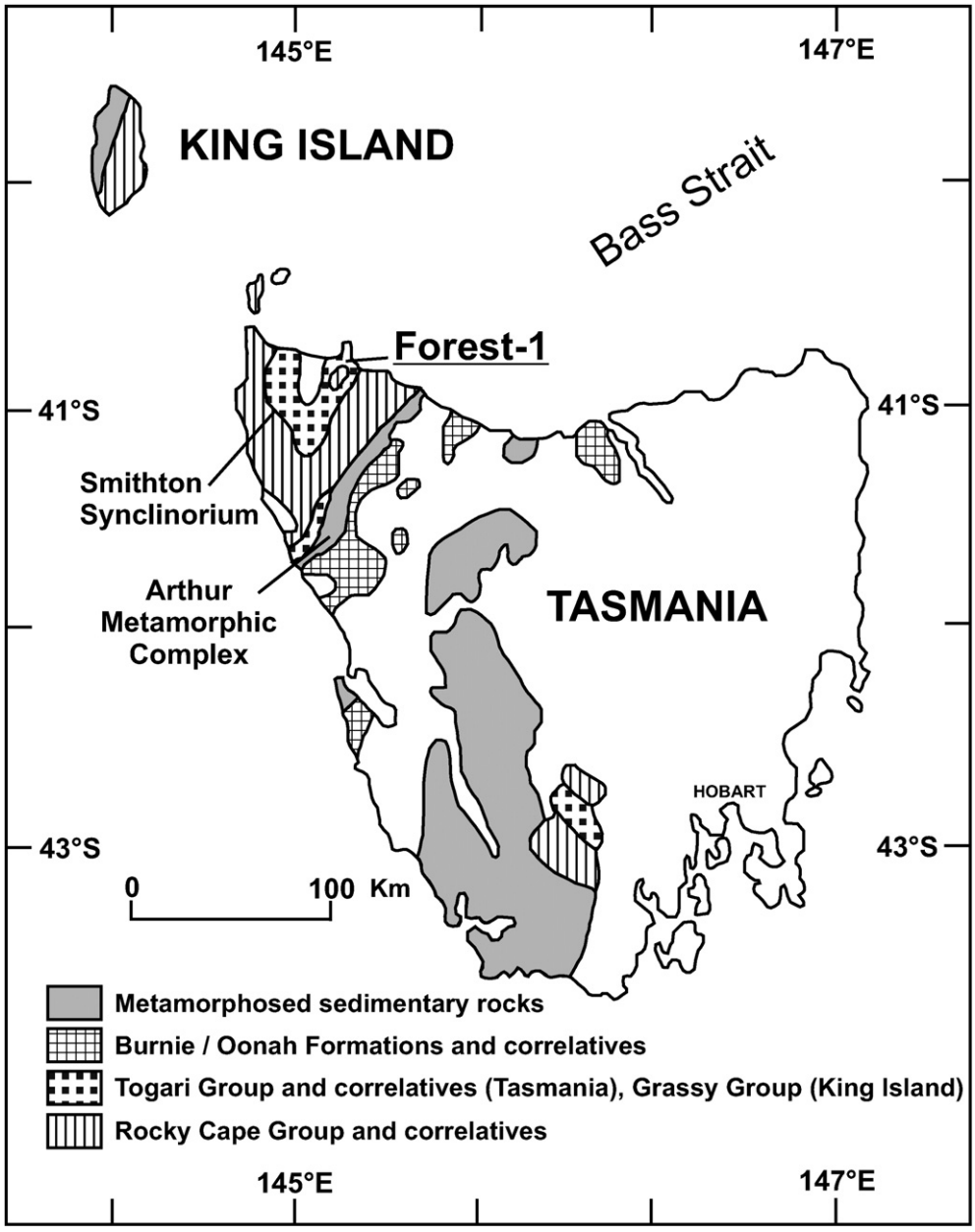

Fig. 1. Simplified geological map showing the distribution of Neoproterozoic rocks in Tasmania and the location of drill hole Forest-1. Modified from Calver and Walter (2000).

(Calver et al., 2004). This reddening of an otherwise organic-rich, ferrous-dominated succession bears similarity to the hypothesized global changes in sulfur (Fike et al., 2006) and iron (Canfield et al., 2007) cycling that accompanied deep ocean oxygenation after the ca. 580 Ma "Gaskiers" glaciation (Bowring et al., 2003; Calver et al., 2004).

The depositional age of the Togari Group is poorly constrained. Detrital zircons in the Forest Conglomerate yield predominantly Paleoproterozoic U–Pb zircon ages (2.5–1.4 Ga; Berry et al., 2001). The underlying Rocky Cape Group has a maximum depositional age of ca. 1000 Ma based on the youngest U–Pb detrital zircon age (Black et al., 2004). Possible correlatives of the Rocky Cape Group in the highly deformed Arthur Metamorphic Complex are older than granitoids dated at 777 ± 7 Ma (U–Pb SHRIMP zircon) that intrude this complex (Turner et al., 1998). Deformed turbidites of the Oonah Formation, southeast of the Arthur Metamorphic Complex, have a wide range of Paleoproterozoic to Mesoproterozoic detrital U–Pb zircon ages (youngest ages are ca. 1280 Ma; Black et al., 2004), a detrital K–Ar muscovite age of 708 ± 6 Ma (Turner, 1993) and a K–Ar biotite age of 725 ± 35 Ma from the syn-depositional Cooee Dolerite (McDougall and Leggo, 1965; revised by Crook, 1979). However, the K–Ar ages may reflect thermal resetting of isotopic systematics and thus the Oonah Formation may be correlative with the Rocky Cape Group (Black et al., 2004). The most reliable radio-isotopic age determination from the Togari Group is a U–Pb SHRIMP zircon age of 582 ± 4 Ma from rhyodacite underlying the Croles Hill Diamictite (Calver et al., 2004).

3. Samples and analytical methods

In the Forest-1 drill core (145°15.3′E, 40°48.9′S; Department of Mines and Mineral Resources, Tasmania core library, Hobart, Tasmania), the Julius River Member is ~130 m thick and comprises two diamictite horizons separated by ~15 m of limestone and subordinate organic-rich shale (Fig. 3). Fine-grained organic-rich dolostone caps the Julius River Member, and is somewhat similar to dolostone

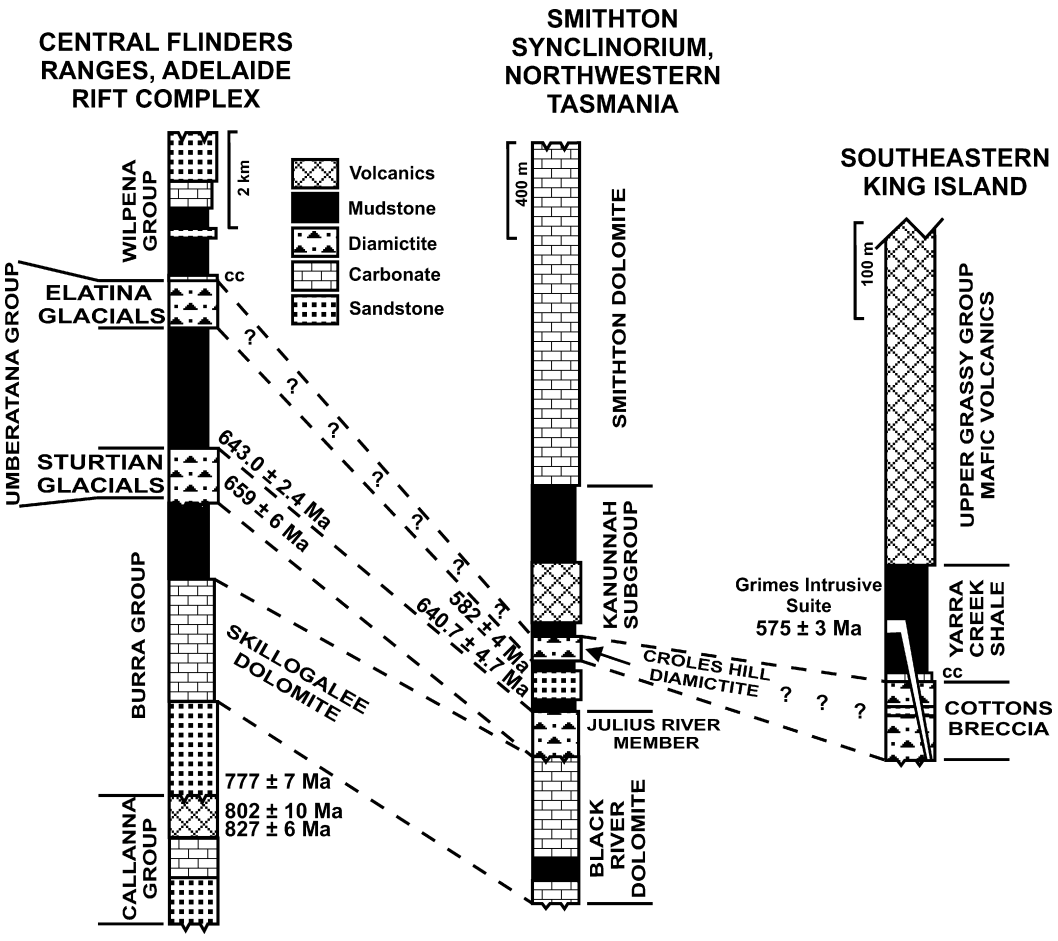

Fig. 2. Generalized stratigraphic columns for southern Australia, northwestern Tasmania, and southeastern King Island showing age constraints and correlations ("cc" denotes cap carbonate). Radio-isotopic age constraints from Wingate et al. (1998) and Fanning et al. (1986) (U–Pb zircon, Callana Group), Preiss (2000) (U–Pb zircon, Burra Group), Fanning and Link (2008) (U–Pb zircon, Sturtian glacials), Kendall et al. (2006) (Re–Os shale, Sturtian post-glacial shale), Calver et al. (2004) (U–Pb zircon, Kanunnah Subgroup and Grimes Intrusive Suite), and this study (Re–Os shale, Black River Dolomite). Modified from Calver and Walter (2000).

lens-bearing sections of the Tindelpina Shale Member (Calver and Walter, 2000), but dissimilar to low-angle, cross-bedded, peloidal cap carbonates found conformably overlying many Elatina Formation glaciogenic diamictites and in rare instances, Sturtian iron formation in southern Australia (Preiss, 1985; Raub et al., 2007). The succeeding ~40 m of strata comprises pyritic black shale with subordinate carbonate, and is lithologically similar to the basal Tindelpina Shale Member (Calver and Walter, 2000). Overlying the black shales are fine-grained volcaniclastic mudstones that grade up-section into volcaniclastic sandstones (Keppel Creek Formation, Kanunnah Subgroup; Calver, 1998; Calver and Walter, 2000). Ten samples of finely laminated pyritic black shale were obtained from 835.58 to 835.87 m depth in Forest-1 and are located ~1 m above the apparently conformable contact with underlying Julius River Member diamictites.

Neoproterozoic rocks from the Smithton Synclinorium have undergone minimal thermal alteration (Calver, 1998; Turner et al., 1998). X-ray diffraction analysis of sample RC06-FOR-01-E yields the mineral assemblage quartz + feldspar + muscovite + dolomite + kaolinite + pyrite. In Forest-1, organic carbon $\delta^{13}C$ is between −34‰ and −24‰, and $\Delta^{13}C_{carbonate\text{-}organics}$ is 28–35 ‰ (Calver, 1998). The latter is similar to the average fractionation of 30‰ for the past 800 M.y. (Hayes et al., 1999). Sub-greenschist facies metamorphism is thus inferred for the Neoproterozoic succession in Forest-1 because greenschist facies metamorphism typically results in $\delta^{13}C_{org}$ heavier than −20‰ and lower $\Delta^{13}C_{carbonate\text{-}organics}$ (Hoefs and Frey, 1976; Hayes et al., 1983).

Between 25 g and 50 g of drill core material was ground to remove cutting and drilling marks, broken into small chips without metal contact, and powdered in an agate mill. Preparation of large powder aliquots (i.e., >20 g) is necessary to avoid any small-scale post-depositional diffusion and/or decoupling of Re and Os in otherwise pristine organic-rich sedimentary rocks (Kendall et al., in press). Rhenium–osmium isotope analyses were carried out at the Radiogenic Isotope Facility of the Department of Earth and Atmospheric Sciences, University of Alberta.

Between 0.45 g and 0.55 g of powder and a known quantity of a ^{185}Re–^{190}Os tracer were digested in 8 mL of Cr^{VI}-H_2SO_4 solution (containing 0.25 g of CrO_3 per 1 mL of 4N H_2SO_4) in sealed Carius tubes for 48 h. This whole-rock digestion protocol minimizes release of detrital Re and Os from the shale silicate matrix by selectively releasing into solution the hydrogenous Re and Os associated with organic matter (Selby and Creaser, 2003; Kendall et al., 2004). In this study, we explored the possibility of using a lower Carius tube digestion temperature (80 °C) rather than the standard temperature of 240 °C to decrease the risk of Carius tube rupture during sample digestion and further minimize acid attack on detrital silicate material (the Cr^{VI}-H_2SO_4 solution does not quantitatively exclude dissolution of silicate minerals; Ravizza et al., 1991; Azmy et al., 2008). Osmium was separated from the Cr^{VI}-H_2SO_4 solution by solvent extraction using chloroform, back-extracted into concentrated HBr, and purified by double micro-distillation (Cohen and Waters, 1996; Birck et al., 1997). Rhenium was separated from the Cr^{VI}-H_2SO_4 solution by anion exchange chromatography (after first

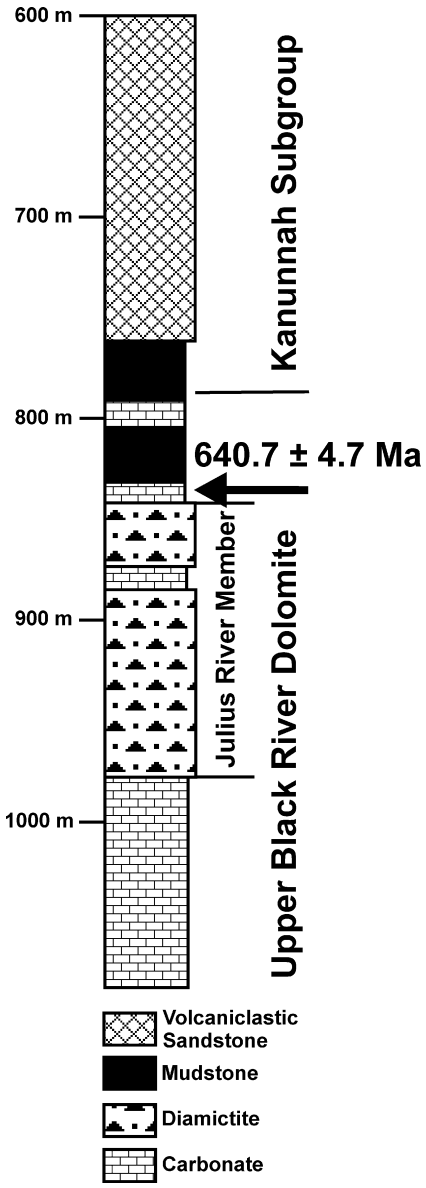

Fig. 3. Stratigraphic column for drill hole Forest-1, Smithton Synclinorium, NW Tasmania. The sample interval used for determining the Re–Os depositional age for the upper Black River Dolomite is shown by the arrow. Modified from Calver (1998).

bubbling in SO_2 gas to reduce Cr^{6+} to Cr^{3+}), and further purified by single bead anion exchange chemistry (Selby and Creaser, 2003). Rhenium and Os were then loaded onto crimped Ni and Pt filaments, respectively (Kendall et al., 2009). Average procedural blanks for Re and Os were 10.8 ± 1.5 pg (1σ, $n=9$) and 0.12 ± 0.05 pg (1σ, $n=8$), respectively, with blank $^{187}Os/^{188}Os$ of 0.24 ± 0.08 (1σ, $n=8$).

Rhenium and osmium abundances and isotope compositions were determined by isotope dilution–negative thermal ionization mass spectrometry (ID-NTIMS) on a Micromass Sector 54 mass spectrometer using Faraday collectors in static mode (for Re) and a pulse-counting electron multiplier in single-collector peak hopping mode (for Os). Isobaric interference of $^{187}ReO_3^-$ on $^{187}OsO_3^-$ at mass 235 was monitored using mass 233 ($^{185}ReO_3^-$), but was determined to be negligible (typically <5 cps). Metal isotope ratios were obtained by correcting raw Re and Os oxide isotopic ratios for isobaric oxygen interferences. Further corrections were made for instrumental mass fractionation (using $^{185}Re/^{187}Re = 0.59738$ and $^{192}Os/^{188}Os = 3.08261$; Nier, 1937; Gramlich et al., 1973), and blank and spike abundances. In-house standard solutions of Re (AB-1) and Os (AB-2) were used to assess long-term instrument reproducibility and yielded values for $^{185}Re/^{187}Re$ and $^{187}Os/^{188}Os$ of 0.59889 ± 0.00044 (1σ, $n=43$) and 0.1069 ± 0.0001 (1σ, $n=46$), respectively, over a seven month interval. Statistically indistinguishable averages for these standard solutions were reported in previous publications by the Radiogenic Isotope Facility at Alberta (e.g., Creaser et al., 2002; Selby and Creaser, 2003; Kendall et al., 2004, 2009; Selby et al., 2005; Azmy et al., 2008). Further, Selby (2007) determined identical values for AB-1 ($^{185}Re/^{187}Re = 0.5977 \pm 0.0012$; 1σ, $n=8$) and AB-2 ($^{187}Os/^{188}Os = 0.1068 \pm 0.0001$; 1σ, $n=6$) from the Arthur Holmes Isotope Laboratory at Durham University.

Re–Os isochron regressions were performed with *Isoplot V.3.0* (Ludwig, 2003) using a value of 1.666×10^{-11} year^{-1} for $\lambda^{187}Re$ (Smoliar et al., 1996; Selby et al., 2007), 2σ uncertainties for $^{187}Re/^{188}Os$ and $^{187}Os/^{188}Os$ determined by error propagation (Kendall et al., 2004), and the error correlation ρ ('rho') (Kendall et al., 2004; Azmy et al., 2008). Use of ρ for black shale Re–Os isochron regressions is recommended because the error correlation between $^{187}Re/^{188}Os$ and $^{187}Os/^{188}Os$ is usually significant (0.37–0.52 in this case).

4. Results

Rhenium (19–39 ppb) and Os (328–525 ppt) abundances of organic-rich shales from the upper Black River Dolomite are significantly elevated relative to average upper crust abundances of ~1 ppb and 30–50 ppt, respectively (Esser and Turekian, 1993; Peucker-Ehrenbrink and Jahn, 2001; Hattori et al., 2003; Sun et al., 2003) (Table 1). The $^{187}Re/^{188}Os$ isotope ratios range between 533 and 832, whereas $^{187}Os/^{188}Os$ isotope ratios range between 6.74 and 9.95. Regression of all Re–Os isotope data yields a Re–Os age of 640.7 ± 4.7 Ma (2σ, $n=19$, Model 1, Mean Square of Weighted Deviates [MSWD] = 0.91, initial $^{187}Os/^{188}Os = 1.00 \pm 0.05$; Fig. 4). Separate regressions of the Re–Os isotope data derived using 240 °C and 80 °C Carius tube digestions yields statistically identical Re–Os ages of 642.7 ± 6.9 Ma (2σ, $n=11$ [10 samples plus 1 replicate analysis], Model 1, MSWD = 0.69, initial $^{187}Os/^{188}Os = 0.98 \pm 0.08$) and 639.3 ± 6.4 Ma (2σ, $n=8$ [7 samples plus 1 replicate analysis], Model 1, MSWD = 1.3, initial $^{187}Os/^{188}Os = 1.02 \pm 0.07$), respectively.

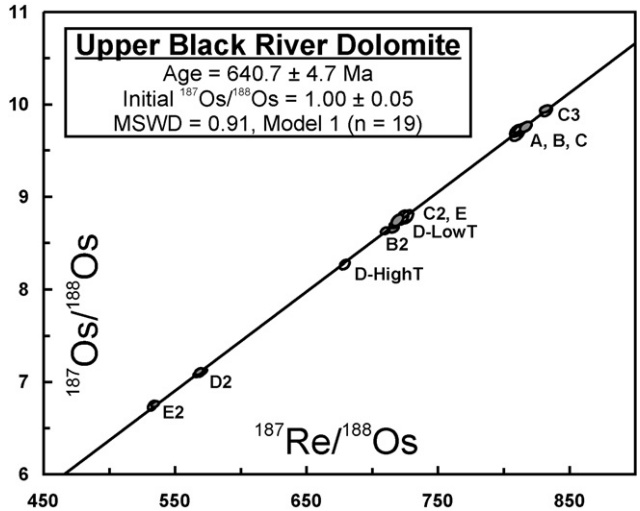

Fig. 4. Re–Os isochron diagram for the upper Black River Dolomite, Togari Group, NW Tasmania. Open and shaded error ellipses denote Carius tube Cr^{VI}-H_2SO_4 digestion at 240 °C and 80 °C, respectively. A Model 1 isochron means the isochron fitting is accomplished by assuming scatter along the regression line is derived only from the input 2σ uncertainties for $^{187}Re/^{188}Os$ and $^{187}Os/^{188}Os$, and ρ.

Table 1
Re–Os data for the upper Black River Dolomite, drill hole Forest-1.

Sample	Depth (m)	Re (ppb)[a]	Os (ppt)[a]	^{192}Os (ppt)[a]	^{187}Re/^{188}Os[a]	^{187}Os/^{188}Os[a]	rho ("ρ")
RC06-FOR-01-A-HighT	835.84–835.87	33.01 (0.11)	440.7 (3.4)	80.8 (0.3)	812.73 (4.12)	9.7250 (0.0538)	0.518
RC06-FOR-01-B2-HighT	835.79–835.84	31.30 (0.10)	448.0 (2.6)	87.7 (0.2)	710.13 (2.91)	8.6322 (0.0303)	0.389
RC06-FOR-01-B2-LowT		31.32 (0.10)	445.2 (2.7)	87.0 (0.2)	716.20 (3.04)	8.6538 (0.0331)	0.419
RC06-FOR-01-B-HighT	835.77–835.79	39.20 (0.13)	524.9 (4.0)	96.3 (0.4)	809.73 (4.04)	9.7128 (0.0534)	0.500
RC06-FOR-01-C3-HighT	835.74–835.77	33.90 (0.11)	447.2 (3.2)	81.0 (0.2)	832.18 (3.63)	9.9297 (0.0467)	0.382
RC06-FOR-01-C3-LowT		33.87 (0.11)	447.7 (2.5)	81.0 (0.2)	831.51 (3.28)	9.9481 (0.0297)	0.373
RC06-FOR-01-C2-HighT	835.72–835.74	31.96 (0.11)	453.4 (3.9)	88.0 (0.3)	722.85 (3.71)	8.7741 (0.0618)	0.421
RC06-FOR-01-C-HighT	835.70–835.72	31.78 (0.11)	424.7 (3.7)	78.0 (0.3)	810.34 (4.43)	9.6873 (0.0675)	0.491
RC06-FOR-01-C-LowT		32.32 (0.11)	430.2 (3.0)	78.7 (0.2)	816.65 (3.64)	9.7570 (0.0440)	0.431
RC06-FOR-01-D2-HighT	835.68–835.70	21.52 (0.07)	347.8 (2.2)	75.2 (0.2)	569.25 (2.54)	7.0957 (0.0319)	0.437
RC06-FOR-01-D2-HighT-rpt		21.41 (0.07)	345.3 (2.0)	74.6 (0.2)	571.22 (2.35)	7.1144 (0.0262)	0.382
RC06-FOR-01-D2-LowT		21.15 (0.07)	342.9 (1.9)	74.2 (0.2)	566.91 (2.37)	7.0857 (0.0256)	0.412
RC06-FOR-01-D2-LowT-rpt		21.48 (0.07)	348.1 (2.1)	75.2 (0.2)	568.29 (2.50)	7.1123 (0.0298)	0.439
RC06-FOR-01-D-HighT	835.65–835.68	27.47 (0.09)	402.0 (2.8)	80.5 (0.2)	678.89 (3.02)	8.2679 (0.0400)	0.398
RC06-FOR-01-D-LowT		28.18 (0.09)	401.3 (2.4)	78.2 (0.2)	716.86 (3.00)	8.7005 (0.0315)	0.416
RC06-FOR-01-E2-HighT	835.62–835.65	19.45 (0.07)	327.9 (2.5)	72.7 (0.3)	532.66 (2.68)	6.7435 (0.0431)	0.440
RC06-FOR-01-E2-LowT		19.62 (0.07)	329.7 (1.9)	73.0 (0.2)	534.79 (2.24)	6.7580 (0.0260)	0.397
RC06-FOR-01-E-HighT	835.58–835.62	28.38 (0.09)	400.9 (3.3)	77.7 (0.3)	726.43 (3.68)	8.7836 (0.0573)	0.438
RC06-FOR-01-E-LowT		28.35 (0.09)	403.6 (3.1)	78.4 (0.3)	719.03 (3.59)	8.7446 (0.0514)	0.468

rpt denotes a replicate analysis. HighT and LowT refer to 48 h Carius Tube digestions at 240 °C and 80 °C, respectively.
[a] Numbers in parentheses denote measured 2σ uncertainty in the abundance or isotope ratio.

The excellent agreement in Re–Os abundance and isotope data obtained by 240 °C and 80 °C Carius tube digestions of the same sample powders (RC06-FOR-01-B2, C, C3, D2, E, and E2) suggests complete equilibration of the spike solution with hydrogenous Re and Os from these shale samples at 80 °C over 48 h. For sample RC06-FOR-01-D, the 240 °C and 80 °C analyses plot on the regression line, but with distinctly different ^{187}Re/^{188}Os and ^{187}Os/^{188}Os ratios, suggesting a non-homogenized powder aliquot after sample processing (Creaser et al., 2002; Kendall et al., 2004). Additional studies on other organic-rich sedimentary rocks are required to determine whether hydrocarbon maturation and/or organic matter composition (Selby and Creaser, 2003) could affect the accuracy and/or precision of Re–Os ages derived using the 80 °C digestion protocol.

5. Discussion

5.1. Correlation of Sturtian and Julius River Member diamictites

A growing body of evidence suggests that the ^{187}Re–^{187}Os radioisotope system represents a precise and accurate deposition-age geochronometer for organic-rich shales that were not subjected to post-depositional alteration by oxidative subaerial and submarine weathering, hydrothermal and diagenetic fluid flow, and metamorphism exceeding the lower greenschist-facies (Kendall et al., in press). Precise depositional ages (better than ± 1%, 2σ) have been obtained for a number of Precambrian organic-rich (TOC ≥ 0.5%) sedimentary rocks (Hannah et al., 2004, 2006; Kendall et al., 2004, 2006; Anbar et al., 2007; Creaser and Stasiuk, 2007; Yang et al., 2009). Concordant U–Pb zircon and Re–Os black shale ages obtained for the Devonian-Mississippian Exshaw Formation (Selby and Creaser, 2005) and the Late Archean Mt. McRae Shale (Anbar et al., 2007) demonstrate the accuracy of the Re–Os deposition-age geochronometer (Kendall et al., in press).

Given the excellent linear fit of the regression (MSWD = 0.91), the Re–Os age of 640.7 ± 4.7 Ma is interpreted as a depositional age for the upper Black River Dolomite. The Re–Os age comes from a ~30 cm interval of organic-rich shale that is ~1 m stratigraphically above the Julius River Member. If an unconformity is absent between the Julius River Member and the overlying organic-rich shale, the Re–Os age of 640.7 ± 4.7 Ma then represents a close minimum age constraint for the depositional age of the Julius River Member.

The Re–Os age for the upper Black River Dolomite is identical (within 2σ uncertainties) to the Re–Os age of 643.0 ± 2.4 Ma for the Sturtian post-glacial Tindelpina Shale Member of southern Australia (Kendall et al., 2006). The Tindelpina Shale Member Re–Os age was obtained from shales stratigraphically located ~3–8 m (based on two drill core sections; Kendall et al., 2006) above the conformable contact with underlying Sturtian glaciogenic diamictites. Notwithstanding major differences in diamictite unit thickness and the general lack of evidence for glaciation in the Julius River Member, the Re–Os shale ages suggest the Julius River Member and Sturtian diamictites and overlying shale units are correlative, consistent with previous lithostratigraphic and stromatolite biostratigraphic evidence (Calver, 1998; Calver and Walter, 2000) (see Fig. 2).

On the basis of carbonate carbon isotope and lithological similarities, the Skillogalee Dolomite (Burra Group) has been correlated with Black River Dolomite carbonates underlying the Julius River Member diamictites (Schidlowski et al., 1975; Veizer and Hoefs, 1976; Belperio, 1990; Calver, 1998). The depositional age of the Skillogalee Dolomite is constrained between 659 ± 6 Ma (U–Pb zircon age from a tuffaceous horizon in the lower Wilyerpa Formation; Fanning and Link, 2008) and 777 ± 7 Ma (U–Pb zircon age from volcanics at the base of the Burra Group; Preiss, 2000). Because the Skillogalee Dolomite is separated from the Sturtian glacial deposits by ~2–3 km of sedimentary rocks, a major unconformity is inferred to be present at the base of the Julius River Member and may be time-correlative with the regional erosional unconformity between the upper Burra Group and Sturtian glacial deposits in the Adelaide Rift Complex (Preiss, 1990, 2000; Calver, 1998). The karst/regolith atop lower Black River Dolomite at the type section of the Julius River Member (Julius River, southern Arthur Forest, Tasmania) may mark this unconformity.

The sub-Julius River unconformity complicates attempts at determining the age of vase-shaped microfossils (VSMs) preserved in chert facies of the lower Black River Dolomite. The VSMs represent the remains of testate amoebae (Porter and Knoll, 2000) and the taphonomic window favouring abundant preservation of these fossils may have occurred during early Neoproterozoic time (Porter, 2006), possibly associated with the appearance and radiation of marine, heterotrophic eukaryotes (Porter and Knoll, 2000). The minimum age for this taphonomic window is poorly constrained, but may be a U–Pb zircon age of 742 ± 6 Ma from an ash bed in the upper Walcott Member of the Kwagunt Forma-

tion, at the top of the Chuar Group in the Grand Canyon, USA (Karlstrom et al., 2000). If deposition of the Black River Dolomite was generally continuous, then the upper Black River Dolomite Re–Os shale age of 640.7 ± 4.7 Ma suggests the lower Black River Dolomite VSMs represent a much younger assemblage relative to other preserved Neoproterozoic VSMs, thus limiting the utility of these fossils for global biostratigraphy. A long-lived unconformity between the lower Black River Dolomite and Julius River Member diamictites, however, permits an early Neoproterozoic age for the lower Black River Dolomite VSMs.

5.2. Os isotope composition of local seawater during Sturtian post-glacial sedimentation

The initial $^{187}Os/^{188}Os$ isotope composition from a black shale Re–Os isochron regression records the contemporaneous local seawater Os isotope composition at the time of sediment deposition (Ravizza and Turekian, 1992; Cohen, 2004; Ravizza and Paquay, 2008; Kendall et al., in press). The radiogenic Os isotope composition ($^{187}Os/^{188}Os$ = 1.00 ± 0.05 and 0.95 ± 0.01 from the upper Black River Dolomite and Tindelpina Shale Member, respectively) of Sturtian post-glacial seawater in the Adelaide Rift Complex and near the Western Tasmania Terrane are similar to present-day seawater ($^{187}Os/^{188}Os$ = 1.06; Peucker-Ehrenbrink and Ravizza, 2000). Thus, riverine inputs of radiogenic Os from oxidative weathering and erosion of upper continental crust (present-day average $^{187}Os/^{188}Os$ of ~1.5; Levasseur et al., 1999) dominated over the influx of unradiogenic Os from cosmic dust and hydrothermal alteration of oceanic crust and peridotites (present-day average $^{187}Os/^{188}Os$ ~0.13; Walker et al., 2002a,b). Post-glacial weathering of crustal material may have resulted in an elevated riverine flux and/or increased riverine $^{187}Os/^{188}Os$ from the continents into local seawater near the margin of the East Antarctic-Australia block following Sturtian glaciation. Similar explanations have been proposed to explain radiogenic seawater Os isotope compositions observed for Cenozoic post-glacial/inter-glacial intervals (Peucker-Ehrenbrink and Blum, 1998; Ravizza and Peucker-Ehrenbrink, 2003; Williams and Turekian, 2004; Dalai et al., 2005, 2006).

5.3. Croles Hill Diamictite–Elatina Formation–Cottons Breccia correlation?

Because the shales immediately overlying the Sturtian and Julius River Member diamictites are demonstrably time-correlative, it is tempting to also correlate the younger diamictite interval in the upper Togari Group (Croles Hill Diamictite) with the glaciogenic Elatina Formation in the Adelaide Rift Complex (see Fig. 2). The Croles Hill Diamictite has a maximum depositional age of 582 ± 4 Ma based on U–Pb SHRIMP zircon dating of underlying rhyodacite, but the Elatina Formation is not geochronologically constrained. In southeastern King Island, sills of the Grimes Intrusive Suite, dated at 575 ± 3 Ma by the U–Pb SHRIMP zircon method, intrude diamictite (Cottons Breccia), and overlying "cap carbonate" (Cumberland Creek Dolostone) and shale (Yarra Creek Shale) (Calver et al., 2004). Correlation of the Cottons Breccia and Elatina Formation is also supported by the similar petrology and carbon isotope chemostratigraphic profiles of the overlying "Marinoan-type" cap carbonates (Cumberland Creek Dolostone and Nuccaleena Formation, respectively), and by post-glacial, organic-rich microbialite facies (Yarra Creek Shale and Brachina Formation, respectively) (Calver, 2000; Calver and Walter, 2000; Preiss, 2000; Corsetti and Lorentz, 2006). Based on their generally similar stratigraphic settings and U–Pb SHRIMP zircon ages, Calver et al. (2004) suggest the Croles Hill Diamictite, Cottons Breccia, and Elatina Formation are correlative with each other and the ca. 580 Ma Gaskiers glacial deposits of eastern Canada (Bowring et al., 2003).

However, this correlation scheme remains uncertain for a number of reasons. For example, a glacial origin for the Croles Hill Diamictite is uncertain, and the time interval between deposition of the Cottons Breccia and emplacement of the 575 ± 3 Ma Grimes Intrusive Suite is not known. The Julius River Member itself does not contain compelling evidence for a glacial influence on deposition, though it is most likely correlative with the Sturtian glacial deposits based on identical Re–Os ages from the immediately overlying shale units. The presence or absence of clear glacial indicators in a diamictite unit does not of itself indicate synchronous or diachronous deposition of diamictite units. Similarly, the absence of a "Marinoan"-type cap carbonate above the Croles Hill Diamictite does not preclude correlation with the Cottons Breccia or Elatina Formation (Calver et al., 2004), but the presence of such carbonates need not uniquely indicate synchronous deposition of underlying diamictite intervals (see below for further discussion). It remains possible that the Elatina Formation and the Cottons Breccia could be older than the <582 ± 4 Ma Croles Hill Diamictite, and instead correlative with ca. 635 Ma glacial deposits of the Nantuo Formation, southern China (Condon et al., 2005) and Ghaub Formation, Namibia (Hoffmann et al., 2004). Accepting this correlation requires very rapid basin evolution in southern Australia (where >4 km of inter-glacial strata are preserved between the Elatina Formation and the 643.0 ± 2.4 Ma Sturtian post-glacial Tindelpina Shale Member; Preiss et al., 1998) and a short duration (<10 M.y.) for the "Snowball" or "Slushball" glaciation ending at ca. 635 Ma. Although rapid basin subsidence and sedimentation rates near basin margins have been inferred for the Central Flinders Zone of the Adelaide Rift Complex (Eyles et al., 2007), only precise radio-isotopic age determinations for the Cottons Breccia and Elatina Formation will firmly resolve this debate. New U–Pb zircon ages from ash beds near the base (636.3 ± 4.9 Ma) and below the unconformable contact (654.5 ± 3.8 Ma) of the Nantuo Formation in southern China do permit the possibility of a <10 M.y. global glaciation (Zhang et al., 2008).

5.4. Ambiguity of "Sturtian"-type cap carbonates as global chronostratigraphic marker horizons

Current global correlation schemes for Neoproterozoic glacial deposits depend heavily upon correlation of two distinctive types of diamictite–cap carbonate pairs that were designated "Sturtian"-type and "Marinoan"-type after the archetypal occurrences in southern Australia. "Marinoan"-type cap carbonates are similar to the Nuccaleena Formation overlying the glaciogenic Elatina Formation in southern Australia. These cap carbonates are characterized by a negative and declining upward $\delta^{13}C$ chemostratigraphic profile, low-angle cross-bedded, peloidal dolomicrite of typically pinkish-cream color, and unusual sedimentary structures such as pseudoteepees, aragonite or barite pseudomorph crystal fans, sheet crack-filling isopachous cements, and tubestones (Kennedy et al., 1998; Hoffman and Schrag, 2002; Halverson et al., 2005; Corsetti and Lorentz, 2006).

Recently, Corsetti and Lorentz (2006) tested the hypothesis that "Marinoan" diamictite–cap carbonate pairs are chronostratigraphic marker horizons. "Marinoan"-type cap carbonates with radio-isotopic age control (Table 2) occur above glaciogenic intervals of: (1) the Scout Mountain Member, Pocatello Formation, Idaho, USA (constrained between U–Pb SHRIMP zircon ages of 701 ± 4 Ma and 667 ± 5 Ma; Fanning and Link, 2004, 2008), (2) Ghaub Formation, Namibia (younger than a U–Pb TIMS zircon age of 635.51 ± 0.54 Ma from an ash bed within the diamictite; Hoffmann et al., 2004), (3) Nantuo Formation, South China (U–Pb TIMS zircon age of 635.23 ± 0.57 Ma from an ash bed within the cap carbonate; Condon et al., 2005), and (4) Icebrook Formation, northwestern Canada (older than a Re–Os black shale age of 607.8 ± 4.7 Ma from the post-glacial Old Fort Point Formation, a possible lithostrati-

Table 2
Summary of cap carbonates with geochronological constraints.

Diamictite unit	Location	Method	Cap characteristics	Minimum age (Ma)	Direct age (Ma)	Maximum age (Ma)	Reference
Macaúbas Group	Brazil	Pb–Pb carbonate (Sete Lagoas Formation)	Sturtian/Marinoan		740 ± 22		Babinski et al. (2007)
Ghubrah Formation	Oman	U–Pb TIMS zircon (tuffaceous bed in diamictite)	Sturtian			714.2 ± 0.6	Bowring et al. (2007)
Pocatello Formation, Scout Mountain Member	Idaho, USA	U–Pb SHRIMP zircon (tuffaceous beds)	Marinoan	667 ± 5		701 ± 4	Fanning and Link (2004, 2008)
Tiesiao Formation	South China	U–Pb TIMS zircon (tuffaceous bed, Datangpo Formation)	Sturtian		662.9 ± 4.3		Zhou et al. (2004)
Areyonga Formation	Central Australia	Re–Os black shale (Aralka Formation)	Sturtian		657.2 ± 5.4		Kendall et al. (2006)
Yudnamutana Subgroup (Sturtian)	South Australia	Re–Os black shale (Tindelpina Shale Member)	Sturtian/Marinoan		643.0 ± 2.4		Kendall et al. (2006)
Ghaub Formation	Namibia	U–Pb TIMS zircon (tuffaceous bed in diamictite)	Marinoan			635.51 ± 0.54	Hoffmann et al. (2004)
Nantuo Formation	South China	U–Pb TIMS zircon (tuffaceous bed, Doushantuo Formation)	Marinoan		635.23 ± 0.57		Condon et al. (2005)
Ice Brook Formation, Stelfox Member	NW, Canada	Re–Os black shale (correlative Old Fort Point Formation)	Marinoan	607.8 ± 4.7			Kendall et al. (2004)

graphic equivalent to the Icebrook Formation cap carbonate and overlying marine shales; Kendall et al., 2004). The Scout Mountain cap carbonate is apparently older than the other "Marinoan"-type cap carbonates by at least 30 M.y. The cap carbonates above the Nantuo Formation and Ghaub Formation (and perhaps the Icebrook Formation) may have been deposited synchronously as part of a global oceanographic event in the aftermath of a "snowball" or "slushball" Earth ice age, but the exact mode of origin for "Marinoan"-type cap carbonates remains contentious (Fairchild and Kennedy, 2007, and references therein).

In their analysis, Corsetti and Lorentz (2006) mention examples of radio-isotopically well-constrained "Sturtian"-type cap carbonates, but do not discuss the time span of deposition for such carbonates nor the Re–Os age for the Sturtian post-glacial Tindelpina Shale Member. We expand upon on their analysis for "Sturtian"-type cap carbonates with accumulating geochronological evidence that the "Sturtian" glaciation was either long-lasting, but diachronous, or there were multiple episodes of glaciation between 750 Ma and 643 Ma, of as yet unknown duration and extent (Kendall et al., 2006). Classic "Sturtian"-type cap carbonates are organic-rich and rhythmically laminated, sometimes contain roll-up structures, and have a carbon isotope profile characterized by initially negative $\delta^{13}C$ values becoming more positive up-section (Kennedy et al., 1998; Hoffman and Schrag, 2002; Halverson et al., 2005; Corsetti and Lorentz, 2006). In addition to examples above some Sturtian glacial deposits (constrained to be 643.0 ± 2.4 Ma from Re–Os dating of the basal Tindelpina Shale Member; Kendall et al., 2006), such carbonates also occur above glaciogenic deposits of the Ghubrah Formation, Oman (younger than a U–Pb TIMS zircon age of 714.2 ± 0.6 Ma from an ash bed within the diamictite; Bowring et al., 2007), the Tiesiao Formation, South China (U–Pb TIMS zircon age of 662.9 ± 4.3 Ma from an ash bed within the cap carbonate; Zhou et al., 2004), and the Areyonga Formation, central Australia (Re–Os black shale age of 657.2 ± 5.4 Ma from the base of the overlying Aralka Formation; Kendall et al., 2006). These examples of "Sturtian"-type cap carbonate deposition span as much as ~70 M.y. of geological time. Even within a single continental block, "Sturtian"-type cap carbonate deposition may be diachronous (e.g., mainland Australia; Kendall et al., 2006). The Sete Lagoas cap carbonate (depositional age of 740 ± 22 Ma based on Pb–Pb dating of well-preserved carbonates) above the Bambuí Group glaciogenic deposits in Brazil has an upward increasing carbon isotope profile (characteristic of "Sturtian"-type caps), but contains aragonite pseudomorph crystal fans (characteristic of "Marinoan"-type caps) (Babinski et al., 2007). Finally, in the structural moat of the syndepositional, "Worumba" salt-withdrawal anticline of South Australia, Waraco Formation dolostone occupies the stratigraphic position of the Tindelpina Shale Member and conformably overlies the Sturtian Holowilena Ironstone (Preiss, 1985). The dolostone is cream-colored and comprises low-angle, cross-bedded peloidal dolomicrite as is typical of "Marinoan" caps, further undermining the utility of distinctive diamictite–cap carbonate pairs as reliable chronostratigraphic marker horizons.

Given the pitfalls associated with carbon isotope chemostratigraphy and the plausible diachronicity of "Sturtian"- and "Marinoan"-type diamictite–cap carbonate pairs, efforts at developing a reliable Neoproterozoic chronostratigraphy should focus on further acquisition of precise and accurate radio-isotopic ages. These radio-isotopic ages could potentially be used to anchor a high-resolution $^{87}Sr/^{86}Sr$ chemostratigraphic curve (e.g., Halverson et al., 2007) and/or a well-established acritarch biostratigraphy (e.g., Willman and Moczydlowska, 2008), although the utility of the latter beyond the Ediacaran Period remains to be established.

6. Conclusions

A new Re–Os depositional age of 640.7 ± 4.7 Ma (Model 1, MSWD = 0.91) is presented for the upper Black River Dolomite (Togari Group, northwestern Tasmania) that provides a close minimum age constraint on deposition of the underlying Julius River Member diamictites. The Re–Os age for the Black River Dolomite is also statistically identical (within 2σ uncertainties) to the Re–Os age of 643.0 ± 2.4 Ma (Model 1, MSWD = 1.1) for the basal Tindelpina Shale Member (Umberatana Group, Adelaide Rift Complex, southern Australia) that overlies Sturtian glaciogenic deposits. Consistent with previous lithostratigraphic and stromatolite biostratigraphic evidence, the Re–Os ages suggest broadly synchronous deposition of the Julius River Member and Sturtian diamictites and immediately overlying organic-rich marine shale successions. Geochronological constraints do not support the use

of "Sturtian-type" diamictite–cap carbonate pairs as chronostratigraphic marker horizons.

Acknowledgements

The manuscript benefited from insightful comments by David Selby and Tony Prave. This research was supported by a Natural Sciences and Engineering Research Council (NSERC) Discovery Grant to Creaser and an Alberta Ingenuity Fund Ph.D. Studentship to Kendall, a David and Lucile Packard Foundation Fellowship to Evans, and by NSF-EAR 0739105 (Raub). Calver publishes with the permission of the Director, Mineral Resources Tasmania. The Radiogenic Isotope Facility at the University of Alberta is supported in part by an NSERC Major Resources Support Grant. Jaime Hallowes and Gayle Hatchard are thanked for technical assistance.

References

Anbar, A.D., Duan, Y., Lyons, T.W., Arnold, G.L., Kendall, B., Creaser, R.A., Kaufman, A.J., Gordon, G.W., Scott, C., Garvin, J., Buick, R., 2007. A whiff of oxygen before the Great Oxidation Event? Science 317, 1903–1906.

Azmy, K., Kendall, B., Creaser, R.A., Heaman, L., Misi, A., de Oliveira, T.F., 2008. Global correlation of the Vazante Group, São Francisco Basin, Brazil: Re–Os and U–Pb radiometric age constraints. Precam. Res. 164, 160–172.

Babinski, M., Vieira, L.C., Trindade, R.I.F., 2007. Direct dating of the Sete Lagoas cap carbonate (Bambuí Group, Brazil) and implications for the Neoproterozoic glacial events. Terra Nova 19, 401–406.

Belperio, A.P., 1990. Palaeoenvironmental interpretations of the Late Proterozoic Skillogalee Dolomite in the Willouran Ranges, South Australia. In: Jago, J.B., Moore, P.S. (Eds.), The Evolution of a Late Precambrian–Early Palaeozoic Rift Complex: The Adelaide Geosyncline. Geol. Soc. Aust. Spec. Publ. 16, pp. 85–104.

Berry, R.F., Jenner, G.A., Meffre, S., Tubrett, M.N., 2001. A North American provenance for Neoproterozoic to Cambrian sandstones in Tasmania? Earth Planet. Sci. Lett. 192, 207–222.

Berry, R.F., Steele, D.A., Meffre, S., 2008. Proterozoic metamorphism in Tasmania: implications for tectonic reconstructions. Precam. Res. 166, 387–396.

Birck, J.L., Roy Barman, M., Capmas, F., 1997. Re–Os isotopic measurements at the femtomole level in natural samples. Geostand. Newslett. 20, 19–27.

Black, L.P., Calver, C.R., Seymour, D.B., Reed, A., 2004. SHRIMP U–Pb detrital zircon ages from Proterozoic and Early Palaeozoic sandstones and their bearing on the early geological evolution of Tasmania. Aust. J. Earth Sci. 51, 885–900.

Bowring, S.A., Myrow, P., Landing, E., Ramenzani, J., 2003. Geochronological constraints on Terminal Neoproterozoic events and the rise of metazoans. Geophys. Res. Abstr. 5, 13219.

Bowring, S.A., Grotzinger, J.P., Condon, D.J., Ramezani, J., Newall, M.J., Allen, P.A., 2007. Geochronologic constraints on the chronostratigraphic framework of the Neoproterozoic Huqf Supergroup, Sultanate of Oman. Am. J. Sci. 307, 1097–1145.

Burrett, C., Berry, R., 2000. Proterozoic Australia–Western United States (AUSWUS) fit between Laurentia and Australia. Geology 28, 103–106.

Calver, C.R., 1998. Isotope stratigraphy of the Neoproterozoic Togari Group, Tasmania. Aust. J. Earth Sci. 45, 865–874.

Calver, C.R., 2000. Isotope stratigraphy of the Ediacarian (Neoproterozoic III) of the Adelaide Rift Complex, Australia, and the overprint of water column stratification. Precam. Res. 100, 121–150.

Calver, C.R., Walter, M.R., 2000. The Late Neoproterozoic Grassy Group of King Island, Tasmania: correlation and palaeogeographic significance. Precam. Res. 100, 299–312.

Calver, C.R., Black, L.P., Everard, J.L., Seymour, D.B., 2004. U–Pb zircon age constraints on Late Neoproterozoic glaciation in Tasmania. Geology 32, 893–896.

Canfield, D.E., Poulton, S.W., Narbonne, G.M., 2007. Late-Neoproterozoic deep-ocean oxygenation and the rise of animal life. Science 315, 92–95.

Cohen, A.S., 2004. The rhenium–osmium isotope system: applications to geochronological and paleoenvironmental problems. J. Geol. Soc. [Lond.] 161, 729–734.

Cohen, A.S., Waters, F.G., 1996. Separation of osmium from geological materials by solvent extraction for analysis by thermal ionisation mass spectrometry. Anal. Chim. Acta 332, 269–275.

Condon, D., Zhu, M., Bowring, S., Wang, W., Yang, A., Jin, Y., 2005. U–Pb ages from the Neoproterozoic Doushantuo Formation, China. Science 308, 95–98.

Corsetti, F.A., Lorentz, N.J., 2006. On Neoproterozoic cap carbonates as chronostratigraphic markers. In: Xiao, S., Kaufman, A.J. (Eds.), Neoproterozoic Geobiology and Paleobiology. Springer, New York, pp. 273–294.

Creaser, R.A., Stasiuk, L.D., 2007. Depositional age of the Douglas Formation, northern Saskatchewan, determined by Re–Os geochronology. In: Jefferson, C.W., Delaney, G. (Eds.), EXTECH IV: Geology and Uranium EXploration TECHnology of the Proterozoic Athabasca Basin, Saskatchewan and Alberta. Geol. Survey Canada Bull. 588, pp. 341–346.

Creaser, R.A., Sannigrahi, P., Chacko, T., Selby, D., 2002. Further evaluation of the Re–Os geochronometer in organic-rich sedimentary rocks: a test of hydrocarbon maturation effects in the Exshaw Formation, Western Canada Sedimentary Basin. Geochim. Cosmochim. Acta 66, 3441–3452.

Crook, K.A.W., 1979. Tectonic implications of some field relationships of the Adelaidean Cooee Dolerite, Tasmania. J. Geol. Soc. Aust. 26, 353–361.

Dalai, T.K., Suzuki, K., Minagawa, M., Nozaki, Y., 2005. Variations in seawater osmium isotope composition since the last glacial maximum: a case study from the Japan Sea. Chem. Geol. 220, 303–314.

Dalai, T.K., Ravizza, G.E., Peucker-Ehrenbrink, B., 2006. The late Eocene $^{187}Os/^{188}Os$ excursion: chemostratigraphy, cosmic dust flux, and the early Oligocene glaciation. Earth Planet. Sci. Lett. 241, 477–492.

Direen, N.G., Crawford, A.J., 2003. Fossil seaward-dipping reflector sequences preserved in southeastern Australia: a 600 Ma volcanic passive margin in eastern Gondwanaland. J. Geol. Soc. [Lond.] 160, 985–990.

Esser, B.K., Turekian, K.K., 1993. The osmium isotopic composition of the continental crust. Geochim. Cosmochim. Acta 57, 3093–3104.

Evans, D.A.D., 2000. Stratigraphic, geochronological, and paleomagnetic constraints upon the Neoproterozoic climatic paradox. Am. J. Sci. 300, 347–433.

Evans, D.A.D., 2006. Proterozoic low orbital obliquity and axial-dipolar geomagnetic field from evaporite palaeolatitudes. Nature 444, 51–55.

Eyles, N., Januszczak, N., 2004. 'Zipper-rift': a tectonic model for Neoproterozoic glaciations during the breakup of Rodinia after 750 Ma. Earth-Sci. Rev. 65, 1–73.

Eyles, C.H., Eyles, N., Grey, K., 2007. Palaeoclimate implications from deep drilling of Neoproterozoic strata in the Officer Basin and Adelaide Rift Complex of Australia; a marine record of wet-based glaciers. Palaeogeog. Palaeoclim. Palaeoecol. 248, 291–312.

Fairchild, I.J., Kennedy, M.J., 2007. Neoproterozoic glaciation in the Earth system. J. Geol. Soc. [Lond.] 164, 895–921.

Fanning, C.M., Link, P.K., 2004. U–Pb SHRIMP ages of Neoproterozoic (Sturtian) glaciogenic Pocatello Formation, southeastern Idaho. Geology 32, 881–884.

Fanning, C.M., Link, P.K., 2008. Age constraints for the Sturtian glaciation: data from the Adelaide Geosyncline, South Australia and Pocatello Formation, Idaho, USA. In: Gallagher, S.J., Wallace, M.W. (Eds.), Neoproterozoic Extreme Climates and the Origin of Early Life, Selwyn Symposium of the GSA Victoria Division. Geol. Soc. Aust. Extended Abstr. 91, pp. 57–62.

Fanning, C.M., Ludwig, K.R., Forbes, B.G., Preiss, W.V., 1986. Single and multiple grain U–Pb zircon analyses for the early Adelaidean Rook Tuff, Willouran Ranges, South Australia. Geol. Soc. Aust. (Abstr.) 15, 71–72.

Fike, D.A., Grotzinger, J.P., Pratt, L.M., Summons, R.E., 2006. Oxidation of the Ediacaran ocean. Nature 444, 744–747.

Giddings, J.A., Wallace, M.W., 2009. Facies-dependant $\delta^{13}C$ variation from a Cryogenian platform margin. South Australia: evidence for stratified Neoproterozoic oceans? Palaeogeog. Palaeoclim. Palaeoecol. 271, 196–214.

Gramlich, J.W., Murphy, T.J., Garner, E.L., Shields, W.R., 1973. Absolute isotopic abundance ratio and atomic weight of a reference sample of rhenium. J. Res. Natl. Bur. Stand. 77A, 691–698.

Griffin, B.J., Preiss, W.V., 1976. The significance and provenance of stromatolitic clasts in a probable late Precambrian diamictite in north-western Tasmania. Papers Proc. R. Soc. Tasmania 110, 111–127.

Halverson, G.P., 2006. A Neoproterozoic chronology. In: Xiao, S., Kaufman, A.J. (Eds.), Neoproterozoic Geobiology and Paleobiology. Springer, New York, pp. 231–271.

Halverson, G.P., Hoffman, P.F., Schrag, D.P., Maloof, A.C., Rice, A.H.N., 2005. Toward a Neoproterozoic composite carbon-isotope record. Geol. Soc. Am. Bull. 117, 1181–1207.

Halverson, G.P., Dudás, F.Ö., Maloof, A.C., Bowring, S.A., 2007. Evolution of the $^{87}Sr/^{86}Sr$ composition of Neoproterozoic seawater. Palaeogeog. Palaeoclim. Palaeoecol. 256, 103–129.

Hannah, J.L., Bekker, A., Stein, H.J., Markey, R.J., Holland, H.D., 2004. Primitive Os and 2316 Ma age for marine shale: implications for Paleoproterozoic glacial events and the rise of atmospheric oxygen. Earth Planet. Sci. Lett. 225, 43–52.

Hannah, J.L., Stein, H.J., Zimmerman, A., Yang, G., Markey, R.J., Melezhik, V.A., 2006. Precise 2004 ± 9 Ma Re–Os age for Pechenga black shale: comparison of sulfides and organic material. Geochim. Cosmochim. Acta 70 (18 (Suppl. 1)), A228.

Hattori, Y., Suzuki, K., Honda, M., Shimizu, H., 2003. Re–Os isotope systematics of the Taklimakan Desert sands, moraines and river sediments around the Taklimakan Desert, and of Tibetan soils. Geochim. Cosmochim. Acta 67, 1195–1205.

Hayes, J.M., Kaplan, I.R., Wedeking, K.W., 1983. Precambrian organic geochemistry, preservation of the record. In: Schopf, J.W. (Ed.), The Earth's Earliest Biosphere: Its Origin and Evolution. Princeton University Press, Princeton, NJ, pp. 93–134.

Hayes, J.M., Strauss, H., Kaufman, A.J., 1999. The abundance of ^{13}C in marine organic matter and isotopic fractionation in the global biogeochemical cycle of carbon during the past 800 Ma. Chem. Geol. 161, 103–125.

Hoefs, J., Frey, M., 1976. The isotopic composition of carbonaceous matter in a metamorphic profile from the Swiss Alps. Geochim. Cosmochim. Acta 40, 945–951.

Hoffman, P.F., Schrag, D.P., 2002. The snowball Earth hypothesis: testing the limits of global change. Terra Nova 14, 129–155.

Hoffman, P.F., Halverson, G.P., Domack, E.W., Husson, J.M., Higgins, J.A., Schrag, D.P., 2007. Are basal Ediacaran (635 Ma) post-glacial "cap dolostones" diachronous? Earth Planet. Sci. Lett. 258, 114–131.

Hoffmann, K.-H., Condon, D.J., Bowring, S.A., Crowley, J.L., 2004. U–Pb zircon date from the Neoproterozoic Ghaub Formation, Namibia: constraints on Marinoan glaciation. Geology 32, 817–820.

Hyde, W.T., Crowley, T.J., Baum, S.K., Peltier, W.R., 2000. Neoproterozoic 'snowball Earth' simulations with a coupled climate/ice-sheet model. Nature 405, 425–429.

Jacobsen, S.B., Kaufman, A.J., 1999. The Sr, C and O isotopic evolution of Neoproterozoic seawater. Chem. Geol. 161, 37–57.

Jiang, G., Kaufman, A.J., Christie-Blick, N., Zhang, S., Wu, H., 2007. Carbon isotope variability across the Ediacaran Yangtze platform in South China: implications

for a large surface-to-deep ocean $\delta^{13}C$ gradient. Earth Planet. Sci. Lett. 261, 303–320.
Karlstrom, K.E., Bowring, S.A., Dehler, C.M., Knoll, A.H., Porter, S.M., Des Marais, D.J., Weil, A.B., Sharp, Z.D., Geissman, J.W., Elrick, M.B., Timmons, J.M., Crossey, L.J., Davidek, K.L., 2000. Chuar Group of the Grand Canyon: record of breakup of Rodinia, associated change in the global carbon cycle, and ecosystem expansion by 740 Ma. Geology 28, 619–622.
Karlstrom, K.E., Åhäll, K.I., Harlan, S.S., Williams, M.L., McLelland, J., Geissman, J.W., 2001. Long-lived (1.8–1.0 Ga) convergent orogen in southern Laurentia, its extensions to Australia and Baltica, and implications for refining Rodinia. Precam. Res. 111, 5–30.
Kaufman, A.J., Knoll, A.H., 1995. Neoproterozoic variations in the C-isotopic composition of seawater: stratigraphic and biogeochemical implications. Precam. Res. 73, 27–49.
Kaufman, A.J., Knoll, A.H., Narbonne, G.M., 1997. Isotopes, ice ages, and terminal Proterozoic Earth history. Proc. Natl. Acad. Sci. 94, 6600–6605.
Kendall, B.S., Creaser, R.A., Ross, G.M., Selby, D., 2004. Constraints on the timing of Marinoan "Snowball Earth" glaciation by ^{187}Re–^{187}Os dating of a Neoproterozoic, post-glacial black shale in Western Canada. Earth Planet. Sci. Lett. 222, 729–740.
Kendall, B., Creaser, R.A., Selby, D., 2006. Re–Os geochronology of postglacial black shales in Australia: constraints on the timing of "Sturtian" glaciation. Geology 34, 729–732.
Kendall, B., Creaser, R.A., Gordon, G.W., Anbar, A.D., 2009. Re–Os and Mo isotope systematics of black shales from the Middle Proterozoic Velkerri and Wollogorang Formations, McArthur Basin, northern Australia. Geochim. Cosmochim. Acta 73, 2534–2558.
Kendall, B., Creaser, R.A., Selby, D. ^{187}Re–^{187}Os geochronology of Precambrian organic-rich sedimentary rocks. In: Craig, J., Thurow, J., Thusu, B., Whitham, A., Abutarruma, Y. (Eds.), Global Neoproterozoic Petroleum Systems: The Emerging Potential in North Africa. Geol. Soc. [Lond.] Spec. Publ., in press.
Kennedy, M.J., Runnegar, B., Prave, A.R., Hoffmann, K.-H., Arthur, M.A., 1998. Two or four Neoproterozoic glaciations? Geology 26, 1059–1063.
Kirschvink, J.L., 1992. Late Proterozoic low-latitude global glaciation: the Snowball Earth. In: Schopf, J.W., Klein, C. (Eds.), The Proterozoic Biosphere. Cambridge University Press, pp. 51–52.
Knauth, P.L., Kennedy, M., 2005. An alternative view of C isotope variations in Neoproterozoic carbonates. Geol. Soc. Am. (Abstr.) 37 (7), 43.
Levasseur, S., Birck, J.-L., Allègre, C.J., 1999. The osmium riverine flux and the oceanic mass balance of osmium. Earth Planet. Sci. Lett. 174, 7–23.
Li, Z.X., Baillie, P.W., Powell, C.McA., 1997. Relationship between northwestern Tasmania and East Gondwanaland in the Late Cambrian/Early Ordovician: Paleomagnetic evidence. Tectonics 16, 161–171.
Lottermoser, B.G., Ashley, P.M., 2000. Geochemistry, petrology and origin of Neoproterozoic ironstones in the eastern part of the Adelaide Geosyncline, South Australia. Precam. Res. 101, 49–67.
Ludwig, K., 2003. Isoplot/Ex Version 3: A Geochronological Toolkit for Microsoft Excel. Geochronology Center, Berkeley.
Maloof, A.C., Kellogg, J.B., Anders, A.M., 2002. Neoproterozoic sand wedges: crack formation in frozen soils under diurnal forcing during a snowball Earth. Earth Planet. Sci. Lett. 204, 1–15.
McDougall, I., Leggo, P.J., 1965. Isotopic age determinations on granitic rocks from Tasmania. J. Geol. Soc. [Aust.] 12, 295–332.
Meert, J.G., 2007. Testing the Neoproterozoic glacial models. Gondwana Res. 11, 573–574.
Meffre, S., Direen, N.G., Crawford, A.J., Kamenetsky, V., 2004. Mafic volcanic rocks on King Island, Tasmania: evidence for 579 Ma break-up in east Gondwana. Precam. Res. 135, 177–191.
Melezhik, V.A., Gorokhov, I.M., Kuznetsov, A.B., Fallick, A.E., 2001. Chemostratigraphy of Neoproterozoic carbonates: implications for 'blind dating'. Terra Nova 13, 1–11.
Nier, A.O., 1937. The isotopic constitution of osmium. Phys. Rev. 52, 885.
Peucker-Ehrenbrink, B., Blum, J.D., 1998. Re–Os isotope systematics and weathering of Precambrian crustal rocks: implications for the marine osmium isotope record. Geochim. Cosmochim. Acta 62, 3193–3203.
Peucker-Ehrenbrink, B., Ravizza, G., 2000. The marine osmium isotope record. Terra Nova 12, 205–219.
Peucker-Ehrenbrink, B., Jahn, B.-M., 2001. Rhenium–osmium isotope systematics and platinum group element concentrations: loess and the upper continental crust. Geochem. Geophys. Geosys. 2, Paper 2001GC000172.
Porter, S.M., 2006. The Proterozoic fossil record of heterotrophic eukaryotes. In: Xiao, S., Kaufman, A.J. (Eds.), Neoproterozoic Geobiology and Paleobiology. Springer, New York, pp. 1–21.
Porter, S.M., Knoll, A.H., 2000. Testate amoebae in the Neoproterozoic Era: evidence from vase-shaped microfossils of the Chuar Group, Grand Canyon. Paleobiology 26, 345–370.
Preiss, W.V., 1985. Stratigraphy and tectonics of the Worumba Anticline and associated intrusive breccias. South Aust. Geol. Survey Bull. 52, 85.
Preiss, W.V., 1990. A stratigraphic and tectonic overview of the Adelaide Geosyncline, South Australia. In: Jago, J.B., Moore, P.S. (Eds.), The Evolution of a Late Precambrian–Early Paleozoic Rift Complex: The Adelaide Geosyncline. Geol. Soc. Aust. Spec. Publ. 16, pp. 1–33.
Preiss, W.V. (compiler), 1993. Neoproterozoic. In: Drexel, J.F., et al. (Eds.), The Geology of South Australia, vol. 1. The Precambrian. South Australia Department of Mines and Energy, Geol. Survey South Aust. Bull. 54, pp. 170–203.
Preiss, W.V., 2000. The Adelaide Geosyncline of South Australia and its significance in Neoproterozoic continental reconstruction. Precam. Res. 100, 21–63.
Preiss, W.V., Dyson, I.A., Reid, P.W., Cowley, W.M., 1998. Revision of lithostratigraphic classification of the Umberatana Group. MESA J. 9, 36–42.
Raub, T.D., Evans, D.A.D., Smirnov, A.D., 2007. Siliciclastic prelude to Elatina Nuccaleena deglaciation: lithostratigraphy and rock magnetism of the base of the Ediacaran system. Geol. Soc. [Lond.] Spec. Publ. 286, 53–76.
Ravizza, G., Turekian, K.K., 1992. The osmium isotopic composition of organic-rich marine sediments. Earth Planet. Sci. Lett. 110, 1–6.
Ravizza, G., Paquay, F., 2008. Os isotope chemostratigraphy applied to organic-rich marine sediments from the Eocene-Oligocene transition on the West African margin (ODP Site 959). Paleocean 23, PA2204.
Ravizza, G.E., Zachos, J.C., H.D. Holland, K.K. Turekian (Executive Editors) 2006. Records of Cenozoic ocean chemistry. In: Elderfield, H. (Ed.), In: The Oceans and Marine Geochemistry. Treatise on Geochemistry, vol. 6. Elsevier, Amsterdam, pp. 551–581.
Ravizza, G., Peucker-Ehrenbrink, B., 2003. The marine $^{187}Os/^{188}Os$ record of the Eocene–Oligocene transition: the interplay of weathering and glaciation. Earth Planet. Sci. Lett. 210, 151–165.
Ravizza, G., Turekian, K.K., Hay, B.J., 1991. The geochemistry of rhenium and osmium in recent sediments from the Black Sea. Geochim. Cosmochim. Acta 55, 3741–3752.
Saito, Y., Tiba, T., Matsubara, S., 1988. Precambrian and Cambrian cherts in northwestern Tasmania. Bull. Nat. Sci. Mus., Tokyo C 14, 59–70.
Schidlowski, M., Eichmann, R., Junge, C., 1975. Precambrian sedimentary carbonates: carbon and oxygen isotope geochemistry and implications for the terrestrial oxygen budget. Precam. Res. 2, 1–69.
Schrag, D.P., Hoffman, P., 2001. Life, geology and snowball Earth. Nature 409, 306.
Selby, D., 2007. Direct rhenium–osmium age of the Oxfordian–Kimmeridgian boundary, Staffin Bay, Isle of Skye, UK and the Late Jurassic timescale. Norwegian J. Geol. 87, 291–299.
Selby, D., Creaser, R.A., 2003. Re–Os geochronology of organic-rich sediments: an evaluation of organic matter analysis methods. Chem. Geol. 200, 225–240.
Selby, D., Creaser, R.A., 2005. Direct radiometric dating of the Devonian–Mississippian time-scale boundary using the Re–Os black shale geochronometer. Geology 33, 545–548.
Selby, D., Creaser, R.A., Dewing, K., Fowler, M., 2005. Evaluation of bitumen as a ^{187}Re–^{187}Os geochronometer for hydrocarbon maturation and migration: a test case from the Polaris MVT deposit, Canada. Earth Planet. Sci. Lett. 235, 1–15.
Selby, D., Creaser, R.A., Stein, H.J., Markey, R.J., Hannah, J.L., 2007. Assessment of the ^{187}Re decay constant by cross calibration of Re–Os molybdenite and U–Pb zircon chronometers in magmatic ore systems. Geochim. Cosmochim. Acta 71, 1999–2013.
Smoliar, M.I., Walker, R.J., Morgan, J.W., 1996. Re–Os ages of Group IIA, IIIA, IVA, and IVB iron meteorites. Science 271, 1099–1102.
Sun, W., Bennett, V.C., Eggins, S.M., Kamenetsky, V.S., Arculus, R.J., 2003. Enhanced mantle-to-crust rhenium transfer in undegassed arc magmas. Nature 422, 294–297.
Trindade, R.I.F., Macouin, M., 2007. Palaeolatitude of glacial deposits and palaeogeography of Neoproterozoic ice ages. Comp. Rend. Geosci. 339, 200–211.
Turner, N.J., 1993. K–Ar geochronology in the Arthur Metamorphic Complex, Ahrberg Group and Oonah Formation, Corinna District. Mineral Resources Tasmania Report 1993/12.
Turner, N.J., Black, L.P., Kamperman, M., 1998. Dating of Neoproterozoic and Cambrian orogenies in Tasmania. Aust. J. Earth Sci. 45, 789–806.
Veizer, J., Hoefs, J., 1976. The nature of $^{18}O/^{16}O$ and $^{13}C/^{12}C$ secular trends in sedimentary carbonate rocks. Geochim. Cosmochim. Acta 40, 1387–1397.
Walker, R.J., Horan, M.F., Morgan, J.W., Becker, H., Grossman, J.N., Rubin, A.E., 2002a. Comparative ^{187}Re–^{187}Os systematics of chondrites: implications regarding early solar system processes. Geochim. Cosmochim. Acta 66, 4187–4201.
Walker, R.J., Prichard, H.M., Ishiwatari, A., Pimentel, M., 2002b. The osmium isotopic composition of convecting upper mantle deduced from ophiolite chromites. Geochim. Cosmochim. Acta 66, 329–345.
Walter, M.R., Veevers, J.J., Calver, C.R., Gorjan, P., Hill, A.C., 2000. Dating the 840–544 Ma Neoproterozoic interval by isotopes of strontium, carbon, and sulfur in seawater, and some interpretative models. Precam. Res. 100, 371–433.
Williams, G.A., Turekian, K.K., 2004. The glacial–interglacial variation of seawater osmium isotopes as recorded in Santa Barbara Basin. Earth Planet. Sci. Lett. 228, 379–389.
Williams, G.E., 2008. Proterozoic (pre-Ediacaran) glaciation and the high obliquity, low-latitude ice, strong seasonality (HOLIST) hypothesis: principles and tests. Earth-Sci. Rev. 87, 61–93.
Willman, S., Moczydlowska, M., 2008. Ediacaran acritarch biota from the Giles 1 drillhole, Officer Basin, Australia, and its potential for biostratigraphic correlation. Precam. Res. 162, 498–530.
Wingate, M.T.D., Campbell, I.H., Compston, W., Gibson, G.M., 1998. Ion microprobe U–Pb ages for Neoproterozoic basaltic magmatism in south-central Australia and implications for the breakup of Rodinia. Precam. Res. 87, 135–159.
Yang, G., Hannah, J.L., Zimmerman, A., Stein, H.J., Bekker, A., 2009. Re–Os depositional age for Archean carbonaceous slates from the southwestern Superior Province: challenges and insights. Earth Planet. Sci. Lett. 280, 83–92.
Young, G.M., Gostin, V.A., 1991. Late Proterozoic (Sturtian) succession of the North Flinders Basin, South Australia: an example of temperate glaciation in an active rift setting. Geol. Soc. Am. Spec. Paper 261, 207–222.
Zhang, S., Jiang, G., Han, Y., 2008. The age of the Nantuo Formation and Nantuo glaciation in South China. Terra Nova 20, 289–294.
Zhou, C., Tucker, R., Xiao, S., Peng, Z., Yuan, X., Chen, Z., 2004. New constraints on the ages of Neoproterozoic glaciations in South China. Geology 32, 437–440.